

Foxp3 occupancy and regulation of key target genes during T-cell stimulation**Supplementary Methods and Discussion**

Cell Generation and Culture Conditions

Cell Culture, Stimulation and Analysis of Cytokine Production

Generation of Foxp3-expressing CD4⁺ T-cell Hybridoma Clones

Transgenic Mice

Purification of Primary CD4⁺ T cells

Foxp3 Location Analysis

Chromatin Immunoprecipitation

Antibodies for ChIP

Ten Slide Promoter Array

Selection of Regions and Design of Subsequences

Compiled Probes and Controls

Single Slide Proximal Promoter Array

Array Scanning and Data Extraction

Data Normalization and Analysis

Identification of Bound Regions

Comparing Bound Regions to Known Genes

Control Location Analysis Experiments

Site-Specific PCR Analysis

DNA Motif Analysis

Gene Expression Analysis

Gene Expression Profiling

Expression Data Normalization

Identification of Differentially Expressed Genes

Hierarchical Clustering and Heatmap Display

Real Time RT-PCR

Statistical Significance of List Overlap

Functional Annotation of Gene Lists

Supplementary Notes**Supplementary Figure Legends and Figures S1-S6**

Cell Generation and Culture Conditions

Cell Culture, Stimulation and Analysis of Cytokine Production

CD4⁺ 5B6-2 hybridoma cells expressing a PLP₁₃₉₋₁₅₁-specific TCR, which was kindly provided by Vijay Kuchroo, were cultured in Dulbecco's modified Eagle medium (Invitrogen). Primary murine CD4⁺ T cells were cultured in RPMI-1640 medium (Invitrogen). Media were supplemented with 10% FCS, 2 mM Glutamax, 1 mM HEPES, 1 mM sodium pyruvate, 0.1 mM non-essential amino acids, 0.55 mM 2-mercaptoethanol, 100U/ml penicillin/streptomycin and 0.1 mg/ml gentamycin. For gene expression profiling, real-time RT-PCR, and location analysis, cells were cultured in the absence or presence of 50 ng/ml phorbol 12-myristate 13-acetate (PMA) and 200 ng/ml ionomycin at 37°C and harvested after 6h. Where indicated, cells were preincubated for 1h with 2 μM cyclosporin A. For the analysis of cytokine production of 5B6-2 hybridoma cells, 10 μg/ml brefeldin A was added for the last 4h of 6 and 36h cultures. Cells were harvested at various time points and intracellular cytokine staining was performed using the Cytotfix/Cytoperm kit (Becton Dickinson) according to manufacturer's recommendations and phycoerythrin-conjugated anti-mouse IL-2 (JES6-5H4) and TNF-α (MP6-XT22) antibodies.

Generation of Foxp3-expressing CD4⁺ T-cell Hybridoma Clones

The murine full-length Foxp3 was amplified from cDNA of purified BALB/c CD4⁺CD25⁺ spleen cells using 5'-ATGCCCAACCCTAGGCCAGCCAA-3' as the sense and 5'-TCAAGGGCAGGGATTGGAGCAC-3' as the antisense primers. A minimal Kozak consensus sequence (double-underlined) just upstream of the initiator codon and a FLAG-tag (single-underlined) and were added using 5'-GAATTCACCATGATGGACTACAAGGACGACGACACAAGCCCAACCCTAGGCCAGCCAA-3' as the sense and 5'-GGATC CTCAAGGGCAGGGATTGGAGCAC-3' as the antisense primers. For further cloning sense and antisense primer sequences contained 5' EcoRI and BamHI restriction sites, respectively. Lentiviral vectors encoding the N-terminal FLAG-tagged Foxp3-IRES-GFP or Empty-IRES-GFP control were generated from the pLenti6/V5-D-TOPO vector (Invitrogen). The integrity of cloned cDNA was confirmed by sequencing and sequence comparison to GenBank

accession no. NM_054039. Concentrated culture supernatants of 293FT transfected with lentiviral vectors were used to infect 5B6-2 hybridoma cells. Stably transduced 5B6-2-[Foxp3]-IRES-GFP or 5B6-2-[Empty]-IRES-GFP 5B6-2 hybridoma cell clones were established after flow cytometric single-cell sorting.

Transgenic Mice

TCR-hemagglutinin (TCR-HA) BALB/c mice express a transgenic TCR specific for the H2-IE^d HA₁₀₇₋₁₁₉ peptide. Double-transgenic TCR-HA x pgk-HA mice additionally express the HA protein under the control of the phosphoglycerate kinase (pgk) promoter and are characterized by high frequencies of TCR-HA-expressing T_{reg} cells¹. Mice were bred in the Dana–Farber Cancer Institute animal facility under specific pathogen-free conditions. Animal care and all procedures were in accordance with the guidelines of the Animal Care and Use Committee of the Dana-Farber Cancer Institute.

Purification and FACS analysis of primary CD4⁺ T cells

Single cell suspensions of pooled spleen and lymph node cells were prepared from TCR-HA and TCR-HA x pgk-HA mice for the purification of naïve and T_{reg} cells, respectively. Cells were stained with fluorochrome-conjugated anti-mouse mAbs CD4 (RM4-5), CD25 (PC61) and TCR-HA (6.5). HA₁₀₇₋₁₁₉-specific CD4⁺CD25⁻ naïve T cells and Foxp3-expressing CD4⁺CD25^{high} T_{reg} cells were then purified using a FACSAria cell sorter and FACSDiva software (Becton Dickinson). Cells were ≥98% pure upon re-analysis. Intracellular staining with the anti-mouse/rat mAb FJK-16s (eBioscience) revealed that ~95% of purified TCR-HA⁺CD4⁺CD25^{high} cells express Foxp3. CD4⁺CD25⁻ naïve T cells showed negligible staining for Foxp3 (≤0.5%). For the analysis of Ly6a surface expression on freshly isolated or *in vitro* stimulated antigen-specific T_{eff} and T_{reg} cells, primary T cells were purified as described above and additionally stained using a phycoerythrin-conjugated anti-mouse mAb Ly6a/e (E13-161.7).

Foxp3 Location Analysis

Chromatin Immunoprecipitation

Protocols describing ChIP methods are available from;
http://jura.wi.mit.edu/young_public/hESregulation/ChIP.html.

Briefly, for each location analysis reaction $\sim 10^8$ N-terminal FLAG-tagged Foxp3-IRES-GFP or Empty-IRES-GFP 5B6-2 hybridomas were chemically crosslinked by the addition of 11% formaldehyde solution for 20 min at room temperature. Cells were washed twice with 1 x PBS and pellets were stored at -80°C prior to use. Cells were resuspended, lysed, and sonicated to solubilize and shear crosslinked DNA. We used a Misonix Sonicator 3000 and sonicated at power 7 for 10-18, 20 second pulses (60 second pause between pulses) at 4°C while samples were immersed in an ice bath. The resulting whole cell extract was incubated overnight at 4°C with 100 μl of Dynal Protein G magnetic beads preincubated with 10 μg of the appropriate antibody for at least 4 hrs. Beads were then washed 4 times with RIPA buffer and 1 time with TBS. Bound complexes were eluted from the beads in elution buffer by heating at 65°C with occasional vortexing, and crosslinking was reversed by ~ 6 hour incubation at 65°C . Whole cell extract DNA (reserved from the sonication step) was also treated for crosslink reversal. Immunoprecipitated DNA and whole cell extract DNA were then purified by treatment with RNaseA, proteinase K and multiple phenol:chloroform:isoamyl alcohol extractions. Purified DNA was blunted, ligated to a universal linker and amplified using a two-stage PCR protocol. Amplified DNA was labelled using Invitrogen Bioprime random primer labelling kits (immunoenriched DNA was labelled with Cy5 fluorophore, whole cell extract DNA was labelled with Cy3 fluorophore). Labelled and purified DNA was combined (4–5 μg each of immunoenriched and whole cell extract DNA) and hybridized to arrays in Agilent hybridization chambers for 40 hours at 40°C . Arrays were then washed and scanned.

Antibodies for ChIP

For ChIP experiments, we used Anti-FLAG (Sigma M2) and anti-E2F4 (Santa Cruz 1082) antibodies. E2F4 antibody has been shown to specifically recognize previously reported E2F4 target genes^{2,3}. Anti-FLAG antibody has also been demonstrated to work for chromatin immunoprecipitation⁴.

Ten Slide Promoter Array

This study employed a 10-slide mouse promoter array set that has been used in previously published work⁵. These arrays were designed to contain oligonucleotides that cover approximately 10 kb around the transcription start sites of approximately 16,000 of the best annotated mouse transcription start sites. Arrays were manufactured by Agilent Technologies (www.agilent.com).

Selection of Regions and Design of Subsequences

To define transcription start sites, we first selected transcripts from three of the most commonly used databases for sequence information (Refseq, Ensembl, MGC). Transcription start sites within 500 bp of each other were considered single start sites. To restrict our array to the most likely transcription start sites, we selected only those that were found in at least two of the three databases. We also included microRNAs from the RFAM database.

25 kb of sequence around each transcription start site (20 kb upstream to 5 kb downstream) was initially extracted for analysis from the repeat-masked sequence derived from the May 2004 build of the mouse genome. Because we were balancing feature number, exact number of transcription start sites, tiling density and extent of upstream genomic coverage for our array design, we chose to design oligos across a much larger region than we were likely to fit on the array. Each transcription start site was considered independent, even if the 25 kb region overlapped with the 25 kb region of another transcription start site. While we anticipated not being able to use all of these oligos, this allowed us flexibility in later design steps to add oligos for additional upstream genomic coverage if space became available. The subset of probes from -8 kb to +2 kb was selected for the actual array. We used the program ArrayOligoSelector 10 (AOS; <http://arrayoligosel.sourceforge.net/>) to score 60-mers for every unmasked subsequence greater than 62 bp across all promoter regions. The scores for each oligo were retained but not put through the built-in AOS selection process. Instead, the collection of scored 60-mers was divided by promoter and sorted by genomic position.

Each set of 60-mers was then filtered based on the AOS oligo scoring criteria: GC content, self-binding, complexity and uniqueness. For our most stringent filter, we selected the following ranges for each parameter: GC content between 30 percent and 100 percent, self-binding score less than 100, complexity score less than or equal to 24, uniqueness greater than or equal to -40 .

From this subset of 60-mers, we selected oligos designed to cover the promoter region with an estimated density of one probe every 280 bp. At this point, we restricted oligo selection to those oligos found within the region 8 kb upstream to 2 kb downstream of the transcription start site. To achieve more uniform tiling, we instituted a simple method to find probes within a particular distance from each other. Starting at the upstream end of the region, we selected the first qualified probe and then selected the next qualified probe located 150 bp to 280 bp away. If there were multiple eligible probes, we chose the most distal probe within the 280 bp limit. If no probes were identified within this limit, we continued scanning until we found the next acceptable probe. The process was then repeated with the most recently selected probe until we reached the end of the promoter region.

For regions that were not covered by high quality probes, we returned to the full set of scored 60-mers and filtered using less stringent criteria. This gave us an additional set of 60-mers that we then used to fill gaps in our coverage. After this second pass, we identified gaps in our coverage and added oligos that were properly spaced and best fit our criteria regardless of whether they passed the filter cutoffs. This iterative process gave us a compromise between optimal probe quality and optimal probe spacing.

Compiled Probes and Controls

There are 407,355 features split over 10 arrays. The probes are arranged such that array 1 begins with the first selected transcript start site on the left arm of chromosome 1, array 2 picks up where array 1 ends, array 3 picks up where array 2 ends, and so on. Over 16,000 genes are represented on the arrays and each promoter region corresponding to a unique start site is covered by approximately 25-27 probes. A true average distance

between probes is difficult to calculate due to the presence of large gaps in the probe tiling. Most of these gaps simply represent the distance between the first and last oligos of two different sets of probes designed against two different genes. Other gaps are caused by lack of available sequence information, repeat masking or sequences that are otherwise highly repetitive and not suitable for oligo design.

Several sets of controls were added. A total of 353 oligos representing *Arabidopsis thaliana* genomic sequence were included. These *Arabidopsis* oligos were BLASTed against the mouse genome and do not register any significant hits. These oligos were intended to check background signal. We added a total of 186 oligos representing five proximal promoter regions of genes that are known targets of the transcriptional regulator Oct4 (Pipox, Foxh1, Oct4/Pou5f1, Msh2 and Hoxb1). Each of the four promoters is represented by 21 - 32 different oligos that are evenly positioned across the regions. The oligos for the Hoxb1 region are printed an additional two times. These promoter regions can be used as positive controls. There are 481 gene desert controls. To identify these probes, we identified intergenic regions of 1 Mb or greater and designed probes in the middle of these regions. These are intended to identify genomic regions that are most likely to be unbound by promoter-binding transcriptional regulators (by virtue of their extreme distance from any known gene). We have used these as normalization controls in situations where a factor binds to a large number of promoter regions. There are 224 features printed as intensity controls; 37 oligos are printed twice and 25 of these 37 are printed an additional six times. Based on a limited number of test hybridizations, this set of oligos gives signal intensities that cover the entire dynamic range of the array. Our intention was that this set could serve as a way to normalize intensities across multiple slides throughout the entire signal range. There are 2,256 controls added by Agilent (standard) and the remainder of each array consists of blank spots.

Single Slide Proximal Promoter Array

Anti-FLAG Foxp3 IPs were compared to control IPs (anti-E2F4 in Foxp3⁺ hybridomas, anti-FLAG in empty vector transduced Foxp3⁻ hybridomas) on a single slide array with ~95,000 probes (Supplementary Figure S4). Oligo probes were designed essentially as

described above. Probes were designed to tile the entire genome with 1 probe placed every ~250bp. A subset of these probes, covering 800bp upstream and 200bp downstream of annotated transcriptional start sites, were then selected to cover the proximal promoters of approximately 18,000 genes.

Array Scanning and Data Extraction

Slides were scanned using an Agilent DNA microarray scanner BA. PMT settings were set manually to normalize bulk signal in the Cy3 and Cy5 channel. For efficient batch processing of scans, we used GenePix 6.0 software (Molecular Devices). Scans were automatically aligned and then manually examined for abnormal features. Intensity data were then extracted in batch. The complete ChIP-chip datasets have been submitted to the online data repository ArrayExpress (<http://www.ebi.ac.uk/arrayexpress/>) and are associated with accession code E-TABM-154.

Data Normalization and Analysis

GenePix was used to obtain background-subtracted intensity values for each fluorophore for every feature on the array. To obtain set-normalized intensities we first calculated, for each slide, the median intensities in each channel for a set of control probes that are included on each array. We then calculated the average of these median intensities for the set of 10 slides. Intensities were then normalized such that the median intensity of each channel for an individual slide equalled the average of the median intensities of that channel across all slides.

Each slide contains a set of negative control spots that contain 60-mer sequences that do not cross-hybridize to murine genomic DNA. We calculated the median intensity of these negative control spots in each channel and then subtracted this number from the set-normalized intensities of all other features.

To correct for different amounts of genomic and immunoprecipitated DNA hybridized to the chip, negative control-subtracted median intensity value of the IP enriched DNA channel for the set of intensity control probes described above was then divided by the

median of the genomic DNA channel for the same set of probes. This yielded a normalization factor that was applied to each intensity in the genomic DNA channel.

Because binding events are rare in the genome, DNA fragments can only be enriched using ChIP, and not anti-enriched. Therefore, the distribution of probes that are below the 1:1 axis ($X\text{-score} = 0$) can provide an empirical non-parametric noise distribution for the experiment. For each X score above 0, the probability of enrichment was calculated to be equal to the number of probes with an X score greater than (more enriched) the test score divided by the total number of probes (enriched + noise) with an absolute value of the X score greater than the test score. This calculation removes the assumption that the X scores on a given array are normally distributed.

Identification of Bound Regions

To automatically determine bound regions in the datasets, we developed an algorithm to incorporate information from neighbouring probes. For each 60-mer, we calculated the average X score of the 60-mer and its two immediate neighbours. If a feature was flagged as abnormal during scanning, we assumed it gave a neutral contribution to the average X score. Similarly, if an adjacent feature was beyond a reasonable distance from the probe (1000 bp), we assumed it gave a neutral contribution to the average X score. The distance threshold of 1000 bp was determined based on the maximum size of labelled DNA fragments put into the hybridization. Since the maximum fragment size was approximately 550 bp, we reasoned that probes separated by 1000 or more bp would not be able to contribute reliable information about a binding event halfway between them. This set of averaged values gave us a new distribution that was subsequently used to calculate test statistics for each probe set.

As most probes were spaced within the resolution limit of chromatin immunoprecipitation, we next required that multiple probes in the probe set provide evidence of a binding event. Bound probes were required to have a single probe probability of enrichment and a probe set probability of enrichment greater than 0.95 (5% False Discovery Rate) for high stringency binding calls and .90 (10% False Discovery

Rate) for low stringency binding calls. Individual probe sets that passed these criteria and were spaced closely together were collapsed into bound regions if the centre probes of the probe sets were within 1000 bp of each other.

Comparing Bound Regions to Known Genes

The location of all bound regions was compared to a composite set of transcripts compiled from three databases: RefSeq⁶, Ensembl⁷, and UCSC annotated known genes (<http://genome.ucsc.edu/cgi-bin/hgTrackUi?g=knownGene>) that were associated with Entrez Gene identifiers and miRNAs downloaded from the the RFAM database (<http://www.sanger.ac.uk/Software/Rfam/>). By this method approximately 16,000 Entrez Genes have a least one probe within -8 kb to +2 kb of their transcription start site. All coordinate information was downloaded from the UCSC Genome Browser (NCBI build 6; March 2005). We assigned bound regions to genes when they were within the -8 kb to +2 kb of the transcriptional start site, which is consistent with our array design. We assigned bound regions to microRNAs when they were within 10kb upstream or downstream of the 5' end of the miRNA.

Control Location Analysis Experiments

Control location analysis experiments demonstrate the specificity of our antibodies for the appropriate targets. When Foxp3 location analysis was performed in hybridoma cells that were not transduced with FLAG-tagged Foxp3 almost no enrichment of DNA was detected. Location analysis experiments with anti-E2F4 antibodies identified expected E2f4 targets, which are dissimilar from the Foxp3 targets that were discovered. These control experiments were performed using the single slide proximal promoter arrays.

Site-Specific PCR Analysis

We used site-specific PCR to confirm binding of Foxp3 to a panel of Foxp3 target genes identified by ChIP-chip. A subset of the bound probe sets was selected and primer pairs were designed to amplify a 150-200 bp region around the genomic location of probes that show peak levels of immunoenrichment. PCR was performed on ligation-mediated PCR amplified IP samples (Figure 3c). 10 ng of immunoprecipitated (IP) DNA was used in

PCR reactions. For input whole cell extract (WCE) samples, a range of DNA amounts (90, 30 and 10 ng of DNA) was used. The PCR was performed for 23 cycles and products were visualized on an agarose gel stained with SYBR Gold (Amersham) and quantified using ImageQuant (Amersham). Enrichment ratios shown in Figure 3c were calculated as the ratio of the intensity of the PCR product from 10ng IP DNA to the product from 10ng WCE DNA. Ratios were normalized relative to the ratio observed for the unenriched β actin control. For site-specific PCR in unamplified IP material from cyclosporin A treated cells (Figure S3), ChIP protocol was followed through the proteinase K digestion. For site-specific PCR, 2 μ l of IP material was used. Again, for whole cell extract (WCE) samples a range of DNA amounts (90, 30 and 10 ng of DNA) was used. 28 cycles of PCR were performed and products were visualized on agarose gel with ethidium bromide. For all site-specific ChIP analysis, a region of the β actin promoter where no Foxp3 binding is expected is used as a negative control.

GENE	5' OLIGO	3' OLIGO	SIZE
Itk	GCTGTTCTTCCAGGAGGATG	AGGCTGGCTGATGCTGATAG	190 bp
Jak2	ACGGCAGGACTAATTGTTGC	GAAAGGGGGAGAAAGAGACG	180 bp
Zap70	TCTAGGACAGGAACACATTGG	GTGTCGGGAACACAAGAGGA	158 bp
Ptpn22	TTCTGCCTTTCTTCTGGGAAT	CTAGCGCCTTCCTTTCTCAA	162 bp
Il2	GTCCTCATGGGCTCAACATC	GGGAGGCCAACCTTTGTAAT	156 bp
Pou2af1	TTCATGAGACGGAAACCACA	CACATCTACAGGAGGGAACCA	156 bp
Ly6a	CCCAGCACAGTGGTAAGAGG	GGCAGGGTTTATCACTTGGA	182 bp
Tnfrsf9	TGTGTGTGTGAAGAGGGGTTT	TCCACAGACGTGACAAGGAG	151 bp
CD25	GGGTGAAAAGACAGCTTGGT	GGGTGTGGGATTCACAAATG	151 bp
β Actin	AGGGTACCACCGAAAAGTC	CCCCAAAGGCTGAGAAGTTA	150 bp

DNA Motif Analysis

Discovery of the Foxp3 sequence motif from the ChIP-chip binding data was performed using the THEME algorithm⁸. THEME tests specific, biologically informed hypotheses about a transcription factor's binding specificity and identifies a motif consistent with both the binding data and prior knowledge regarding the protein's DNA-binding domain structural family.

We extracted genomic sequence corresponding to the regions bound by Foxp3 at high confidence in stimulated cells for use as the “foreground” data set in THEME. We then extracted sequence regions at random from unbound regions on the array for use as the “background” data set. The length of these unbound sequences was matched to the average size of the bound set (700bp) to avoid biasing either set towards motif presence or absence. We then ran THEME, testing hypotheses consistent with the Forkhead DNA-binding domain family, and identified the motif that yielded the lowest bound vs. unbound classification error after 5-fold cross-validation. The statistical significance of the best motif’s cross-validation error was assessed by running THEME on randomized data (using the starting hypothesis from which the best motif was derived) and calculating a Z-score for the observed error under the null hypothesis that the sequences were selected at random from the background set. We then tested hypotheses corresponding to 35 other distinct DNA-binding domains in an identical fashion, and found that the best motif identified from the Forkhead family yielded a lower cross-validation error than any motif from all other families tested.

The Foxp3 motif learned by THEME, and the Nfat motif from the TRANSFAC (version 8.3) database⁹ were used to scan all arrayed sequences to identify matches to the motif. Each potential site was assessed by summing the position-specific scores from the motif log-odds matrix. Sites were identified as matches if their score was greater than or equal to the threshold, determined by the THEME algorithm, which classified bound and unbound sequences with the lowest error during motif discovery. For the Nfat motif from TRANSFAC a threshold of 60% of the maximum possible score was used. Foxp3 motif conservation in bound regions was determined using mm6/hg17 mouse-human pairwise alignments obtained from the UCSC Genome Browser¹⁰. If the human sequence directly aligned to the motif match in mouse also met the score threshold we identified that site as a conserved match. We performed the same conservation calculations for randomly selected unbound microarray sequence regions. Statistical significance was determined by fitting a hypergeometric distribution to the data and testing the null

hypothesis that the number of conserved Foxp3 motifs observed in bound regions arose from random selection without replacement from the background population. We then examined the distribution of spacings between Foxp3 and Nfat motifs (when they occurred together in the same Foxp3 bound region). Statistical significance was determined using the hypergeometric test described above. Results are summarized in Supplementary Table S5. The online tool WebLogo (<http://weblogo.berkeley.edu>) was used to generate DNA motif sequence logo in Figure 2b.

Gene Expression Analysis

Gene Expression Profiling

For each hybridoma culture condition, total RNA was prepared from 1×10^7 cells using Trizol (Gibco) followed by additional purification using the RNeasy Mini Kit (Qiagen). Biotinylated antisense cRNA was then prepared according to the Affymetrix standard labelling protocol (one amplification round). For each primary T-cell culture condition, total RNA was isolated from 5×10^5 cells with RNeasy. Biotinylated antisense cRNA was prepared by two rounds of *in vitro* amplification using the BioArray RNA Amplification and Labeling System (Enzo Life Sciences) according to the protocol for 10-1000 ng of input RNA provided by the manufacturer. Biotinylated cRNAs of hybridomas and primary T cells were fragmented and hybridized to Affymetrix GeneChip Mouse Expression Set 430 2.0 arrays at the Microarray Core Facility (Dana-Farber Cancer Institute). Arrays were stained, scanned, and quantified according to standard Affymetrix protocols. Data were annotated according the NetAffx database (<http://www.affymetrix.com/analysis/index.affx>) as of March, 2006. The complete expression datasets have been submitted to the online data repository ArrayExpress (<http://www.ebi.ac.uk/arrayexpress/>) and are associated with accession code E-TABM-154.

Expression Data Normalization

Quantile normalization was performed separately on the hybridoma and *ex vivo* expression datasets. Expression data were ranked within each sample. Within each

sample, each probeset was given a signal value of the average signal of the probesets of that rank, across the dataset.

Identification of Differentially Expressed Genes

The hybridoma dataset was analyzed for statistically significant differential expression using the online NIA Array Analysis Tool¹¹ (<http://lgsun.grc.nia.nih.gov/ANOVA/>).

Probesets were tested for differential expression using the following settings:

Threshold z-value to remove outliers: 10000

Error Model: Max(Average, Bayesian)

Error variance averaging window: 200

Proportion of highest error variances to be removed: 0.01

Bayesian degrees of freedom: 5

FDR threshold: .05

Of 45,101 probesets on the Affymetrix Mouse 430 2.0 array, 256 were differentially expressed between Foxp3⁻ and Foxp3⁺ stimulated hybridomas, while 23 probesets were differentially expressed in the unstimulated cells. The expression data for these probesets are provided (Supplementary Tables S7 and S8). Probesets were excluded that had an average signal intensity that was not in the upper tercile on the arrays (54.4 units). Probesets that did not map to the genes for which we had Foxp3 binding data and probesets that mapped to multiple genes were also excluded. In the cases where multiple probesets mapping to one gene were differentially expressed, only the probeset showing the largest differential expression was displayed.

It is worth noting that a stringent cutoff to call differential expression is used. This identifies expression changes with high confidence but produces an underestimate because there are many genes that show small changes. Our goal is to gain insight into Foxp3 action, and by focusing on only the most pronounced transcriptional effects, we aim to minimize the effects of noise in the expression data. As a result of this approach, some genes that are likely to be regulated directly by Foxp3 exhibit small transcriptional effects that are not called differentially expressed. For example the genes *Bcl10*, *Cd53*, *Rbpsuh*, and *Rgs1* are all direct Foxp3 binding targets that are known to play a role in

regulation of T cells, and have the characteristic expression pattern of suppressed activation, but do not meet the $FDR < 5\%$ statistical significance cutoff for differential expression.

Genes with consistent Foxp3 dependent differential expression between stimulated *ex vivo* T helper and T_{reg} cells and between stimulated Foxp3⁻ and Foxp3⁺ hybridoma cells were determined according to the following method. Probesets were excluded that had an average signal intensity that was smaller than the median signal on the arrays (26.2 units). Probesets that did not map to the genes for which we had Foxp3 binding data and probesets that mapped to multiple genes were also excluded. In the cases where multiple probesets mapping to one gene were differentially expressed, only the probeset showing the largest differential expression was displayed.

A score for Foxp3 dependent differential expression was calculated in the hybridoma and *ex vivo* datasets separately. The product of these scores was used to sort the genes and identify those with the largest Foxp3 dependent differential expression, which was consistent in the two cell types. To calculate each score, the average signal intensity within the two groups being compared was calculated. The difference in signal between the groups being compared was divided by the median signal intensity of all probesets on the array (26.2 units) plus one eighth of the average signal intensity for that probeset.

$$(A - B) / ((A + B) / 2) / 8 + median$$

This generated a differential expression score that is comparable to a signal to noise ratio, where noise is estimated be a linear function of signal intensity. In Supplementary Figure S5, the 125 genes with the highest overall differential expression score were displayed, to match the number of genes that are shown in Figure 3A.

Hierarchical Clustering and Heatmap Display

For clustering and heat map display, expression data were Z-score normalized separately within the hybridoma and *ex vivo* datasets. For heatmap display in Supplementary Figure S5 data were Z-score normalized within the full hybridoma and *ex vivo* datasets including the unstimulated samples, though only the stimulated samples are displayed. Average

linkage, correlation distance, centered, hierarchical clustering was performed using Gene Cluster (<http://bonsai.ims.u-tokyo.ac.jp/~mdehoon/software/cluster/software.htm#ctv>). Heatmaps were generated using Java Treeview (<http://jtreeview.sourceforge.net/>). Cluster branches were flipped about tree nodes for optimal display. In Figure 3B, those genes from panel A that are bound by Foxp3 and are expressed in *ex vivo* cells are displayed in panel B. *Slc17a6* and *Adam10* are excluded because they are not expressed in the *ex vivo* samples.

Real-time RT-PCR

Total RNA was prepared from hybridoma cells or FACS purified primary T-cell populations using the RNeasy kit (Qiagen) followed by DNase digestion (Qiagen). cDNA was synthesized from total RNA using Superscript II reverse transcriptase and oligo(dT) (Invitrogen Life Technologies) according to the manufacturer's recommendations. Real-time RT-PCR was performed on an ABI PRISM thermal cycler (Applied Biosystems) using SYBR[®] Green PCR core reagents (Applied Biosystems). Real-time RT-PCR primer sets were either obtained from SuperArray or are available upon request.

Statistical Significance of List Overlap

Statistical significance of overlap between differentially expressed genes and Foxp3 bound genes was calculated using a standard Chi-Square test.

Functional Annotation and Statistical Significance of Gene Lists

Functional annotation and statistical significance of gene lists was performed with the on-line tool, DAVID (<http://niaid.abcc.ncifcrf.gov/>)¹². Genes were imported as EntrezGene IDs and, using the Functional Annotation tool, compared to KEGG pathways¹³.

The Foxp3 binding targets in PMA/ionomycin-stimulated CD4⁺ hybridomas were enriched for genes associated with the following KEGG pathways:

KEGG Pathway	P-Value
T-CELL RECEPTOR SIGNALING PATHWAY	1.4E-5

CELL CYCLE	4.3E-3
FATTY ACID ELONGATION IN MITOCHONDRIA	2.5E-2
CYTOKINE-CYTOKINE RECEPTOR INTERACTION	5.9E-2
PYRIMIDINE METABOLISM	9.2E-2

The Foxp3 target genes that are downregulated in Foxp3⁺ stimulated hybridomas relative to their levels in Foxp3⁻ stimulated hybridomas were enriched for genes associated with the following KEGG pathways:

KEGG Pathway	P-Value
T-CELL RECEPTOR SIGNALING PATHWAY	6.1E-3
CYTOKINE-CYTOKINE RECEPTOR INTERACTION	3.6E-2

Supplementary Notes

1. Klein, L., Khazaie, K., von Boehmer, H. In vivo dynamics of antigen-specific regulatory T cells not predicted from behaviour in vitro. *Proc. Natl. Acad. Sci.* **100**, 8886-8892 (2003).
2. Ren, B., et al. E2F integrates cell cycle progression with DNA repair, replication, and G(2)/M checkpoints. *Genes Dev.* **16**, 245-256 (2002).
3. Weinmann, A.S., Yan, P.S., Oberley, M.J., Huang, T.H., Farnham, P.J. Isolating human transcription factor targets by coupling chromatin immunoprecipitation and CpG island microarray analysis. *Genes Dev.* **16**, 235-244 (2002).
4. Henry, K.W., et al. Transcriptional activation via sequential histone H2B ubiquitylation and deubiquitylation, mediated by SAGA-associated Ubp8. *Genes Dev.* **17**, 2648-2663 (2003).
5. Boyer, L.A., et al. Polycomb complexes repress developmental regulators in murine embryonic stem cells. *Nature.* **441**, 349-353. (2006).
6. Pruitt, K.D., Tatusova, T. & Maglott, D.R. NCBI Reference Sequence (RefSeq): a curated non-redundant sequence database of genomes, transcripts and proteins. *Nucleic Acids Res* **33**, D501-504 (2005).
7. Hubbard, T. et al. Ensembl 2005. *Nucleic Acids Res* **33**, D447-453 (2005).
8. MacIsaac, K.D., et al. A hypothesis-based approach for identifying the binding specificity of regulatory proteins from chromatin immunoprecipitation data. *Bioinformatics.* **22**, 423-429 (2006).
9. Wingender E., et al. TRANSFAC: a database on transcription factors and their DNA binding sites. *Nucleic Acids Res.* **24**, 238-241 (1996).
10. Karolchik, D., et al. "The UCSC Genome Browser Database." *Nucl. Acids Res* **31**, 51-54 (2003).
11. Sharov, A.A., Dudekula, D.B., Ko, M.S. A web-based tool for principal component and significance analysis of microarray data. *Bioinformatics.* **21**, 2548-2549 (2005).
12. Dennis, G. Jr., et al. DAVID: Database for Annotation, Visualization, and Integrated Discovery. *Genome Biology.* **4**, 3 (2003).
13. Kanehisa, M. & Goto, S. KEGG: Kyoto encyclopedia of genes and genomes. *Nucleic Acids Res.* **28**, 27-30 (2000).

14. Wu, Y., et al. FOXP3 Controls Regulatory T Cell Function through Cooperation with NFAT. *Cell*. **126**, 375-387 (2006).
15. Chen, C., Rowell, E.A., Thomas, R.M., Hancock, W.W., Wells, A.D. Transcriptional regulation by Foxp3 is associated with direct promoter occupancy and modulation of histone acetylation. *J Biol Chem*. (2006).

Supplementary Figure Legends

Figure S1. Flow cytometric analysis of Foxp3 expression. 5B6-2-[Foxp3]-IRES-GFP or 5B6-2-[Empty]-IRES-GFP 5B6-2 hybridoma cells (**a**) or FACS-purified *ex vivo* TCR-HA transgenic CD4⁺CD25⁻ naïve or CD4⁺CD25⁺ Treg cells (**b**) were cultured in the absence or presence of PMA/ionomycin. After 6h cells were harvested and intracellular staining was performed using the mAb FJK16s (anti-Foxp3). Histograms show relative levels Foxp3 protein expression, which demonstrates that Foxp3 is expressed at a similar level in the transduced hybridomas as in *ex vivo* T_{reg} cells.

Figure S2. Cytokine production of Foxp3-transduced 5B6-2 hybridomas. 5B6-2-[empty]-IRES-GFP (**a**) or 5B6-2-[Foxp3]-IRES-GFP (**b**) hybridoma cells were cultured in the presence of PMA/ionomycin for the indicated times. Brefeldin A was added for the last 4h of 6h and 36h cultures. After surface staining for CD4 expression and fixation, intracellular staining with the indicated cytokine antibodies or appropriate isotype controls was performed. Numbers in dot plots indicate the frequencies of cells in the respective quadrant. These data show that Foxp3 transduction suppresses production of IL2, but does not suppress production of TNF- α .

Figure S3. The promoters of most Foxp3 target genes are bound by Foxp3 before and after T-cell stimulation. (**a**) The lists of genes whose promoters are bound by Foxp3 in unstimulated (blue) and stimulated (pink) hybridoma cells are shown in a Venn diagram. The genes occupied by Foxp3 in stimulated T cells (FDR < .05) are represented by the pink circle. The genes occupied by Foxp3 in unstimulated T cells (FDR < .05) are represented by the blue circle. The dotted light blue circle represents the genes occupied by Foxp3 in unstimulated cells if the threshold is relaxed to FDR < .10. Most of the genes bound in stimulated cells are prebound in unstimulated cells. (**b**) Although most Foxp3 bound genes in stimulated cells were also bound in unstimulated cells, the binding profiles were not identical in the two conditions. *Ptpn22* and *Jak2* were representative of target genes where strong immunoenrichment was observed in both conditions. The binding profile for Foxp3 is shown at these promoters with binding in unstimulated cells

displayed with a blue line and binding in stimulated cells displayed with a pink line. The profile across these promoter regions indicates that additional Foxp3 binding events are stabilized in response to PMA/ionomycin stimulation. This phenomenon is observed at several Foxp3 targets. In contrast to the strong immunoenrichment observed in both conditions at *Ptpn22* and *Jak2*, recent reports^{14,15} indicates that Foxp3 is stabilized at the promoters of *Il2* and *CD25* in response to T-cell stimulation. This finding is confirmed in our Foxp3 binding data as shown here. **(c)** Foxp3 binding at the *Ptpn22* and *Jak2* promoters in unstimulated cells was independently confirmed with site-specific ChIP in cyclosporin A treated cells. Primers flanking the binding peaks indicated with asterisks in **(b)** were used for ChIP PCR reactions shown here. Immunoenrichment at the *Ptpn22* and *Jak2* promoters was observed. As expected, immunoenrichment was not observed at the *Il2*, *CD25*, and control *β actin* promoters.

Figure S4. Control experiments confirm the specificity of Foxp3 ChIP-chip. When \log_2 intensity values of IP (Cy5 label) material are plotted against \log_2 intensity values of whole cell extract (Cy3 label), considerable enrichment of IP material is observed in ChIP experiments in FLAG-tagged Foxp3⁺ cells both before **(a)** and after **(b)** PMA/ionomycin stimulation. In contrast, very little IP enrichment is observed when the same IPs are performed in Foxp3⁻ hybridomas **(c)**. A positive control IP with an anti-E2F4 antibody identifies expected IP enriched E2F4 targets **(d)**, which are largely distinct from the identified Foxp3 target genes (see Supplementary Table S4).

Figure S5. Many Foxp3 targets show consistent Foxp3 dependent differential expression in *ex vivo* and hybridoma cells. Genes were selected that showed consistent Foxp3 dependent differential expression in *ex vivo* and hybridoma cells according to methods described in the Supplementary section, Identification of Differentially Expressed Genes. 125 genes are displayed to match the number of genes in Figure 3a. For clustering and heatmap display data were Z-score normalized within the full hybridoma and *ex vivo* datasets including the unstimulated samples, though only the stimulated samples are displayed. Data were hierarchically clustered and are displayed in a heatmap. The Z-score normalized induction (red) or repression (green) is shown for

each gene. Direct targets of Foxp3 are signified with blue bars, with dark blue representing genes called bound with a false discovery rate of 5% and light blue representing a false discovery threshold of 10%. There is a significant enrichment of direct Foxp3 targets among the genes that are downregulated in stimulated Foxp3⁺ cells ($p < 10^{-19}$).

Figure S6. Analysis of Ly6a protein expression on primary T_{reg}. Surface expression of Ly6a on CD4⁺6.5⁺ naïve T cells from TCR-HA mice or Foxp3-expressing CD4⁺CD25^{high}6.5⁺ T_{reg} cells from double-transgenic TCR-HA x pgk-HA mice was analyzed on freshly FACS-purified cells (**a**) or after 18h of culture in the absence or presence of 50 ng/ml PMA and 200 ng/ml ionomycin with or without a 1h preincubation with 2 μM cyclosporin A (**b**).

Figure S1

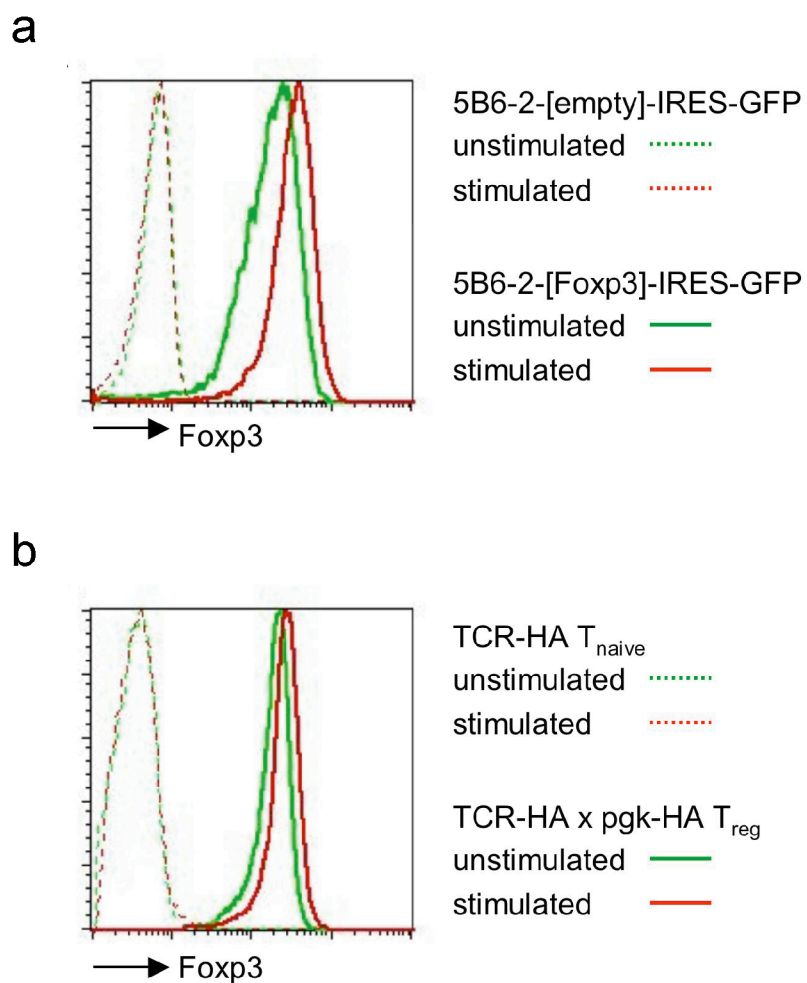
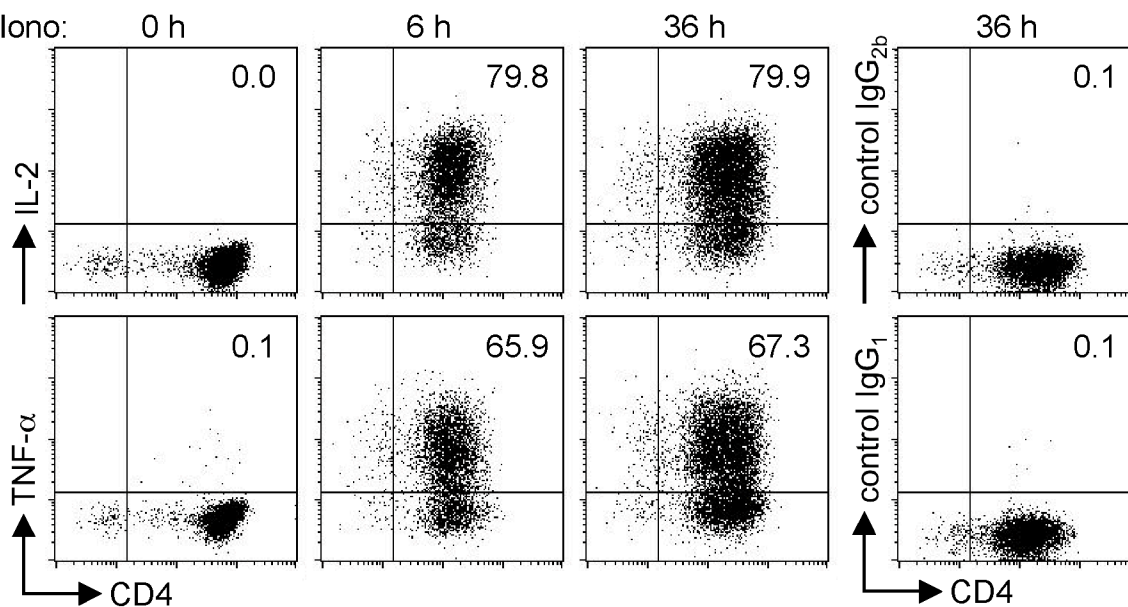


Figure S2

a

5B6-2-[empty]-IRES-GFP:

PMA/Iono:



b

5B6-2-[Foxp3]-IRES-GFP:

PMA/Iono:

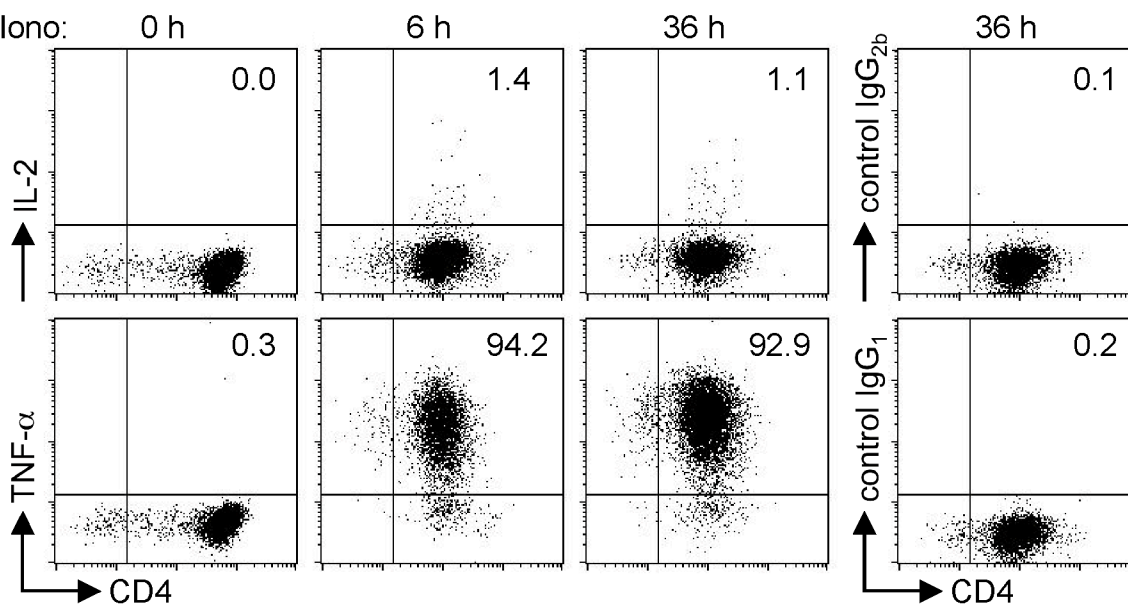


Figure S3

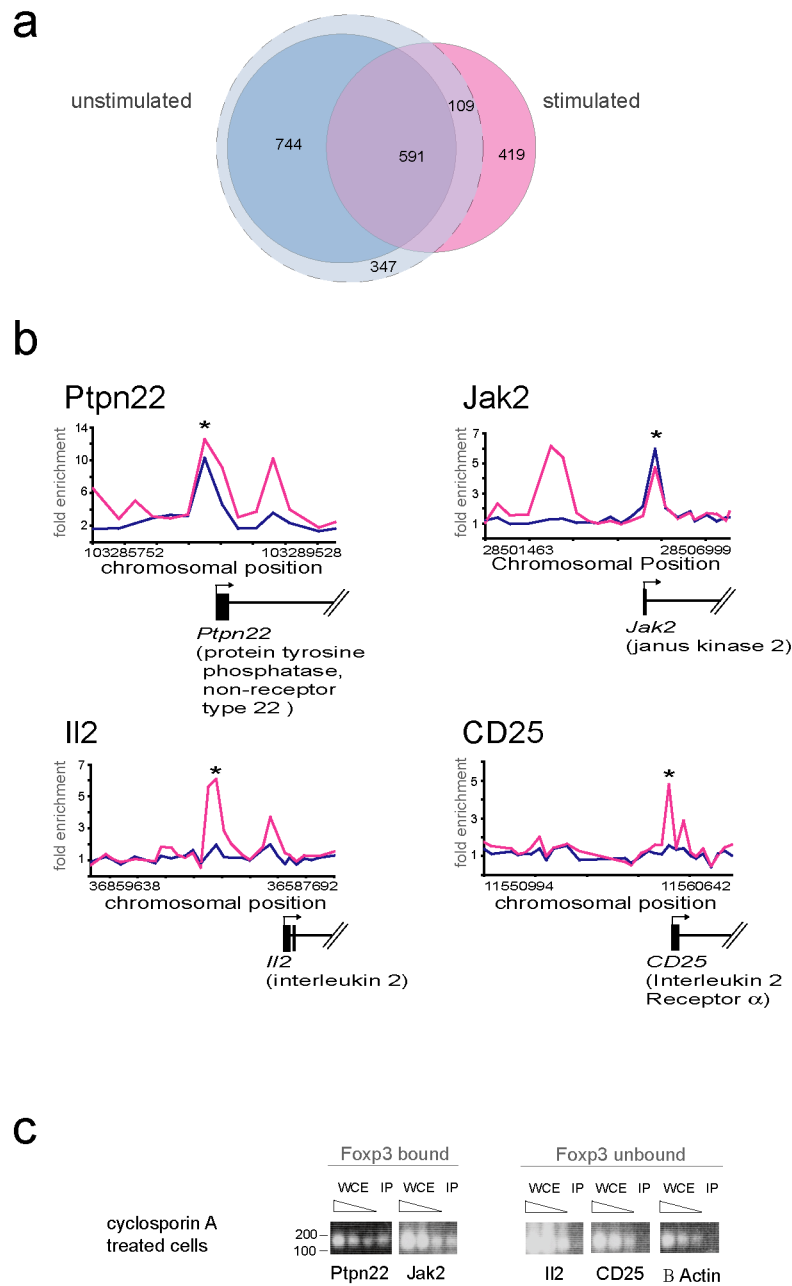


Figure S4

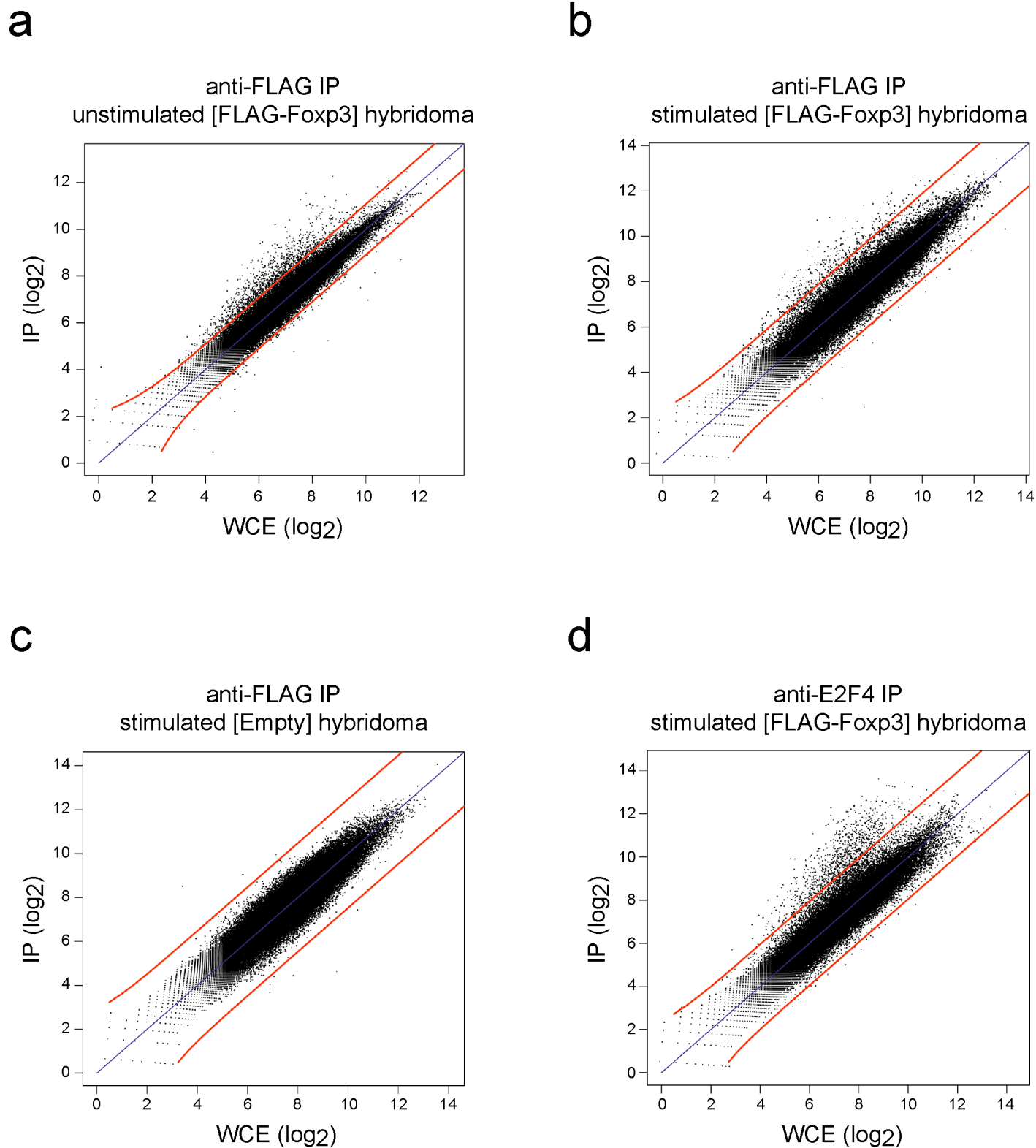


Figure S5

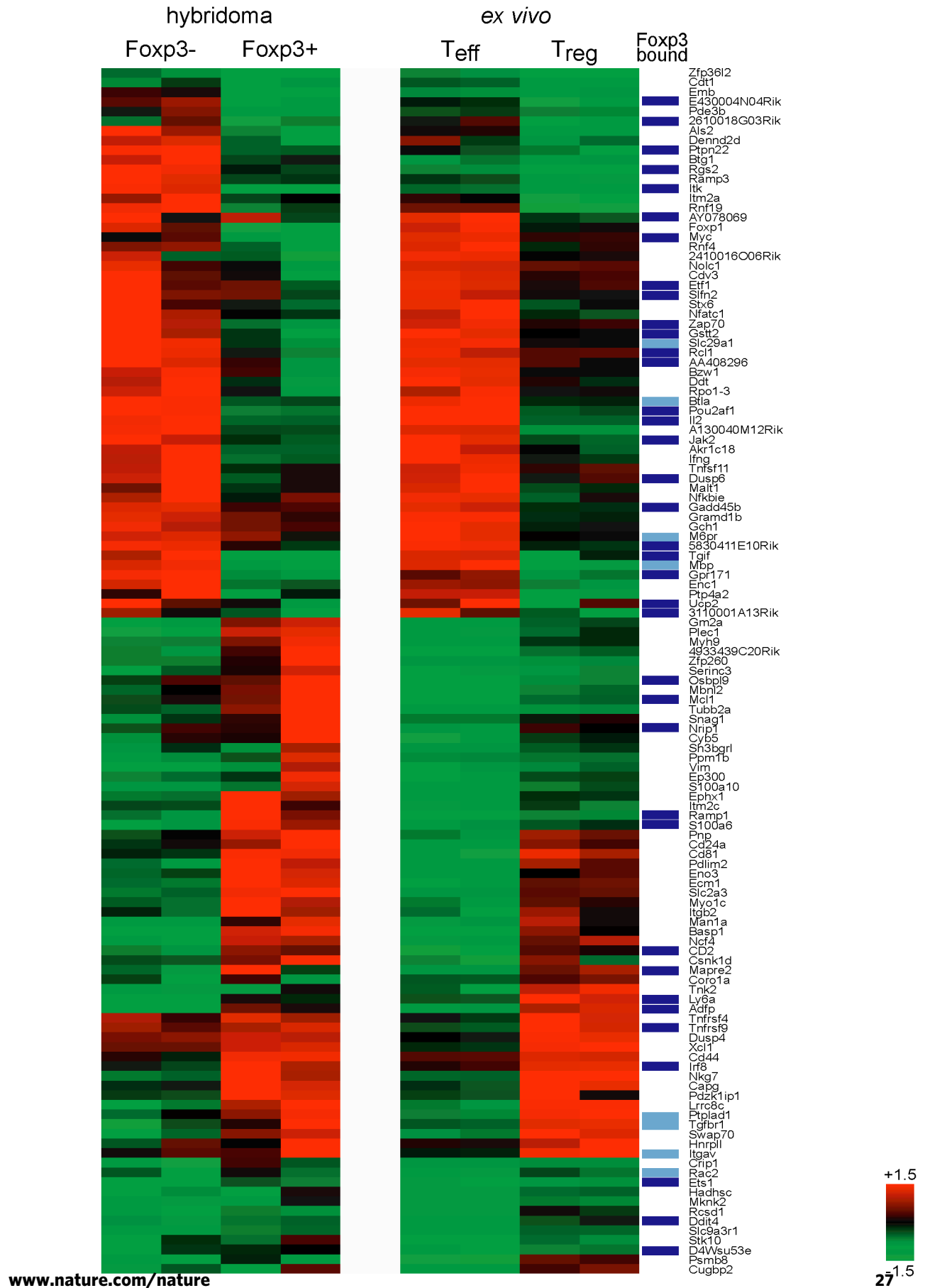
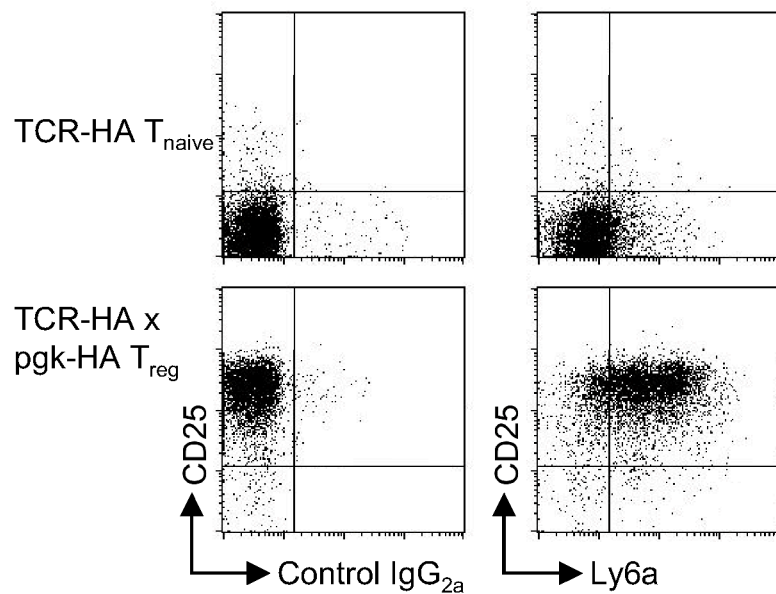


Figure S6

a



b

